J integral computation for piezo-ceramics

Nadia Benkaci — Gérard Maugin

LMM - UMR CNRS 7607
Université Pierre et Marie Curie
8 rue du Capitaine Scott, F-75015 Paris

{Benkaci} benkaci@lmm.jussieu.fr

{Maugin} gam@ccr.jussieu.fr

ABSTRACT. *Piezo-ceramics are brittle; they can fail untimely due to the propagation of flaws or defects produced during their manufacturing process. In this paper, we propose a numerical estimate of a J-integral generalized to electro-mechanical processus, wich will prove useful in designing a propagation criterion. To that end, we use the finite-element method to solve the piezo-electric problem, providing thus displacements and coordinates of elements that constitute the chosen integration path. Then the computation of J is achieved by using the energy-domain-integral method for piezo-ceramics such as PZT-4H and PZT-5H.*

RÉSUMÉ. *Les piézo-céramiques sont des matériaux fragiles; la propagation d'un défaut acquis lors du processus de fabrication peut provoquer une rupture prématurée. Dans cet article, nous proposons un calcul numérique d'une intégrale J generalisée aux processus électro-mécaniques utile dans un critère de propagation. Pou cela, on utilise la méthode des éléments finis pour la résolution du problème piézo-électrique fournissant les déplacements et les coordonnées des différents éléments qui constituent le contour d'intégration. Le calcul numérique de J est effectué par la méthode de l'intégrale du domaine de l'énergie pour des piézo-céramiques PZT-4H et PZT-5H.*

KEYWORDS: *Finite element computation, energy-domain-integral method, piezo-electricity, piezo-ceramics, PZT-4H, PZT-5H.*

MOTS-CLÉS : *Calculs par éléments finis, méthode de l'intégrale du domaine de l'énergie, piézo-électricité, piézo-céramiques, PZT-4H, PZT-5H.*

1. Introduction

Piezoelectricity is a characteristic property of the material which can exist naturally (for example quartz) or can be transmitted artificially to the material by submitting it to polarization. This is the case of the ceramics, for example: barium titanate, lead zirconate or PZT which are the most used piezoelectric ceramics in industrial applications. A non piezoelectric isotropic ceramic, submitted to polarization, becomes an anisotropic piezoelectric one with a transverse elastic isotropy and a hexagonal symmetry of class 6mm with x_3 as an axis of polarization and $x_1 - x_2$ as an isotropic plane. Piezoceramics are brittle [PAK 90] [SUO 92]; the propagation of a flaw or a defect produced during their manufacturing process can cause an early failure. An electrical potential of a magnitude of about MV/m applied to a piezoceramic can enhance the propagation of a crack [CHU 89]. As these materials are frequently used in industry, it becomes necessary to introduce a failure criteria to predict their lasting quality during their life service. The notion of crack extension force is taken as the critical threshold of the fracture. When this extension is along the x_1 axis, this force becomes identical to the J integral. When the traction on the crack faces is zero, we have $G = J$ [PAK 86] [MCC 90].

Up to now, J was calculated with an approximate method [PAK 90] [SUO 92] [SUN 95]. In this study, we intend to compute J numerically for a piezoceramic material. We will adopt the following procedure: the elastic problem will be solved thanks to MODULEF (The program developed by INRIA); this will allow us to have the coordinates, strains and the electric field of the different elements of the path integral, these results will be the input data to our program "rupture" to calculate J by using the energy integral domain method.

2. Problem formulation

For a linear, elastic, piezo-electric, by neglecting the body forces in the small strain theory J is (see [MAU 95], [DAS 94] and [DAS 95])

$$J = \int_{\Gamma} (W\delta_{i1} - \sigma_{ij}u_{j,1} + D_iE_1)n_i d\Gamma \qquad [1]$$

Here Γ is any path surrounding the crack tip, beginning at the inferior crack surface and ending at the superior one in the trigonometric way, the unit normal n_i being oriented outward. W is the electric enthalpy, σ_{ij} is the stress field, and D_{ij} is the electric induction field.

For the calculation of the J integral, we assume the hypothesis of brittle fracture i.e, the material is continuous and elastic in the macroscopic sense but it contains a discontinuity of the displacements. The first step is to solve the electroelastic problem to find out the value of the different contributions in expression 1.

3. Electroelastic problem formulation

3.1. *The case of a piezoelectric material*

For a region B of R^3 occupied by a piezoelectric structure under surface forces of density T^d applied on the ∂B_T part of the boundary ∂B; the displacements are imposed on ∂B_u which is a part of this boundary. In addition, the region B is subject to the electric charges applied on the part ∂B_q^e and to an electric potentiel on ∂B_ϕ^e. The problem is to determine the displacement field u_i and the electric potential ϕ in every point M of B and also the stress field σ and the charge density q from the initial configuration u_0 and ϕ_0. The formulation of the problem with the partial derivatives in the quasistatic case is:

$$\left\{\begin{array}{l}\text{find } u_i(x,y,z) \text{ and } \phi(x,y,z) \text{ on } B \text{ for } i=1,2,3 \text{ with:}\\ \qquad\qquad \sigma_{ij,j} = 0 \quad \text{in } B;\\ \qquad\qquad D_{i,i} = 0 \quad \text{in } B;\\ \qquad\qquad \sigma_{ij} n_j = T_i^d \quad \text{on } \partial B_T;\\ \qquad\qquad D_i n_i = q \quad \text{on } \partial B_q^e;\\ \qquad\qquad u_i = u_i^d \quad \text{on } \partial B_u;\\ \qquad\qquad \phi = \phi^d \quad \text{on } \partial B_\phi^e;\end{array}\right. \qquad [2]$$

with :

- n_i : the unit exterior normal to ∂B;
- u_i^d : the imposed displacement on ∂B_u;
- q : the imposed electric charge on ∂B_q^e;
- ϕ^d : the imposed potential on ∂B_ϕ^e;
- σ_{ij} : the stresses field;
- D_i : the electric displacement.

The constitutive equations of the piezoelectrics are given by:

$$\left\{\begin{array}{l}\sigma_{ij} = C_{ijkl} S_{kl} - e_{mij} E_m \quad \text{and} \quad D_i = e_{ijk} S_{jk} + \epsilon_{il} E_l\end{array}\right. \qquad [3]$$

$S_{ij} = \frac{1}{2}(u_{i,j} + u_{j,i})$ is the strains field, and E_i is the electric field, $E_i = -\phi_{,i}$

Piezoelectricity is a simple generalization of the elastic problem by adding an unknown scalar, the electric potential ϕ. Indeed, the constitutive equations are still in the general linear form (but in a larger space of nine dimensions).

$$\{\sigma\} = [\tilde{C}].\{S\} \qquad [4]$$

With:

$$\begin{array}{l}\{\sigma\} = \{\sigma_{11} \quad \sigma_{22} \quad \sigma_{33} \quad \sigma_{23} \quad \sigma_{13} \quad \sigma_{12} \quad D_1 \quad D_2 \quad D_3\}^T\\ \{S\} = \{s_{11} \quad s_{22} \quad s_{33} \quad s_{23} \quad s_{13} \quad s_{12} \quad -E_1 \quad -E_2 \quad -E_3\}^T\end{array} \qquad [5]$$

and:

$$[\tilde{C}] = \begin{bmatrix} C_{11} & C_{12} & \dots & C_{16} & e_{11} & e_{21} & e_{31} \\ & C_{22} & \dots & C_{26} & e_{12} & e_{22} & e_{33} \\ & & \dots & \dots & \dots & \dots & \dots \\ & & & C_{66} & e_{16} & e_{26} & e_{36} \\ & & & & -\epsilon_{11} & -\epsilon_{12} & -\epsilon_{13} \\ & & & & & -\epsilon_{22} & -\epsilon_{23} \\ & & & & & & -\epsilon_{33} \end{bmatrix} \quad [6]$$

3.2. *The particular case of ceramics*

The constitutive equations for a piezoceramic are:

$$\begin{Bmatrix} \sigma_{11} \\ \sigma_{22} \\ \sigma_{33} \\ \sigma_{32} \\ \sigma_{31} \\ \sigma_{12} \end{Bmatrix} = \begin{bmatrix} c_{11} & c_{12} & c_{13} & 0 & 0 & 0 \\ c_{12} & c_{11} & c_{13} & 0 & 0 & 0 \\ c_{13} & c_{13} & c_{33} & 0 & 0 & 0 \\ 0 & 0 & 0 & c_{44} & 0 & 0 \\ 0 & 0 & 0 & 0 & c_{44} & 0 \\ 0 & 0 & 0 & 0 & 0 & c_{66} \end{bmatrix} \begin{Bmatrix} s_{11} \\ s_{22} \\ s_{33} \\ 2s_{32} \\ 2s_{31} \\ 2s_{12} \end{Bmatrix} - \begin{bmatrix} 0 & 0 & e_{31} \\ 0 & 0 & e_{31} \\ 0 & 0 & e_{33} \\ 0 & e_{15} & 0 \\ e_{15} & 0 & 0 \\ 0 & 0 & 0 \end{bmatrix} \begin{Bmatrix} E_1 \\ E_2 \\ E_3 \end{Bmatrix} \quad [7]$$

$$\begin{Bmatrix} D_1 \\ D_2 \\ D_3 \end{Bmatrix} = \begin{bmatrix} 0 & 0 & 0 & 0 & e_{15} & 0 \\ 0 & 0 & 0 & e_{15} & 0 & 0 \\ e_{31} & e_{31} & e_{33} & 0 & 0 & 0 \end{bmatrix} \begin{Bmatrix} s_{11} \\ s_{22} \\ s_{33} \\ 2s_{32} \\ 2s_{31} \\ 2s_{12} \end{Bmatrix}$$

$$+ \begin{bmatrix} \epsilon_{11} & 0 & 0 \\ 0 & \epsilon_{11} & 0 \\ 0 & 0 & \epsilon_{33} \end{bmatrix} \begin{Bmatrix} E_1 \\ E_2 \\ E_3 \end{Bmatrix} \quad [8]$$

4. Problem of the boundary conditions on the crack faces

Concerning the boundary conditions on the crack faces, Mikhailov and Parton (1990) [MIK 90] and Parton (1976) [PAR 95] have assumed that crack faces to be traction free and that the potential and the normal components of the induction are continuous:

$$\phi^+ = \phi^- \qquad D_n^+ = D_n^- \quad [9]$$

This condition is not physically valid because the permittivity for the piezoceramics is about 10^3 superior to the environment one (example of silicon oil or air) [PAK 90] which does not allow ϕ or D to be continuous across the crack faces.

In 1980, Deeg [DEE 80] analysed the dislocation, fracture and inclusion problems in piezoelectric solids. In order to simplify his study, he assumed that the normal component of the electric induction (on the crack faces) vanishes. PAK [PAK 90] has formulated a detailed argument to justify this hypothesis, that is why this condition is called the D-P condition (Deeg and Pak) [TON 96].

In 1987 [MCM 87], McMeeking has studied the fracture of a dielectric with a conductor fluid filling the crack. He found out that the most appropriate condition is $\phi^+ = \phi^- = 0$.

Actually the D-P condition is the one commonly used in the mechanical study of the fracture of the piezoelectric materials. This hypothesis consists in considering the crack faces traction free and the normal component of the electric induction on the crack faces zero. This condition is valid in the case of imperfect contact of the crack faces and when the space between the two crack faces is filled by air or by a non-conducting gas, this is what happens in reality, especially in the case of a mechanical loading acting in the opening mode of the crack.

5. The energy-domain-integral method

5.1. *The case of an elastic material*

5.1.1. *Two-dimensional problem*

Starting with the expression of the J integral (see [MAU 93], [MAU 95] and [RIC 71]):

$$J = \lim_{\Gamma_0 \to 0} \int_{\Gamma_0} [W\delta_{1i} - \sigma_{ij} \frac{\partial u_j}{\partial x_1}] n_i d\Gamma \qquad [10]$$

We can write equation [10] in a new form by considering a closed contour around the crack tip. The procedure is as follows. Let us note the exterior normal to Γ^* : $\vec{m}$, as in figure 1 ($\Gamma^* = \Gamma_1 - \Gamma_0 + \Gamma^+\Gamma^-$). We have then

on	Γ^+ and Γ^-	:	$m_1 = 0$ and $m_2 = \pm 1$,
on	Γ_0	:	$m_i = -n_i$,
on	Γ_1	:	$m_i = n_i$.

By introducing a fonction q which is smooth in the closed domain and equal to 1 on Γ_0 and 0 on Γ_1, we can easily show that equation [10] takes on the form:

$$J = \int_{\Gamma^*} (\sigma_{ij} \frac{\partial u_j}{\partial x_1} - W\delta_{1i}) q m_i d\Gamma - \int_{\Gamma_+ + \Gamma_-} \sigma_{2j} \frac{\partial u_j}{\partial x_1} q d\Gamma \qquad [11]$$

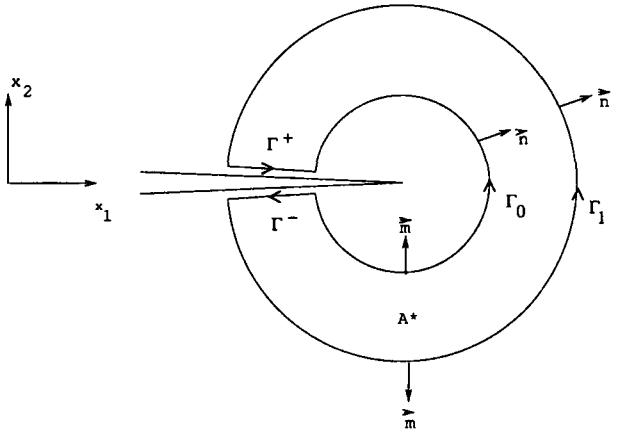

Figure 1. *Representation of the closed contour around the crack tip*

The second term disappears when considering the crack faces traction free. Using the Green-Gauss theorem we can write :

$$J = \int\int_{A^*} \frac{\partial}{\partial x_i} [(\sigma_{ij} \frac{\partial u_j}{\partial x_1} - W\delta_{1i})] q dA$$

$$= \int\int_{A^*} (\sigma_{ij} \frac{\partial u_j}{\partial x_1} - W\delta_{1i}) \frac{\partial q}{\partial x_i} dA$$

$$- \int\int_{A^*} (\frac{\partial W}{\partial x_i}\Big|_{\delta_{A_i}} - \frac{\partial}{\partial x_i}(\sigma_{ij} \frac{\partial u_j}{\partial x_1})) q dA \qquad [12]$$

Here A^* is the area enclosed by Γ_0 and Γ_1. The second term of the integral is zero when the body forces are neglected. For an elastic material under quasistatic conditions, in the absence of the body forces, thermal strains and crack-face traction, equation [12] becomes:

$$J = \int\int_{A^*} (\sigma_{ij} \frac{\partial u_j}{\partial x_1} - W\delta_{1i}) \frac{\partial q}{\partial x_i} dA \qquad [13]$$

Equation [13] is path independent; q can be interpreted as a normalized virtual displacement. That is why the domain integral method is interpreted as a method analogous to the the virtual-crack-extension one.

5.1.2. *Three-dimensional problem*

In the two-dimensional case, the path integral was expressed in terms of an area integral. In the three-dimensional case, it will be more appropriate for the numerical analysis to express the path integral in terms of a volume integral.

In the case of three-dimensional fracture, we introduce a local coordinate system in the position η where $J(\eta)$ is calculated along the crack front as indicated in figure (2a) by using equation [10]. The path Γ_0 is located in the plane $(o, \vec{x_1}, \vec{x_2})$ (see figure 2b).

Let us construct a tube of length ΔL and of radius r_0 along a segment of crack front.

We define the virtual extension of an elementary segment of the crack front as indicated in the figure 3 below.

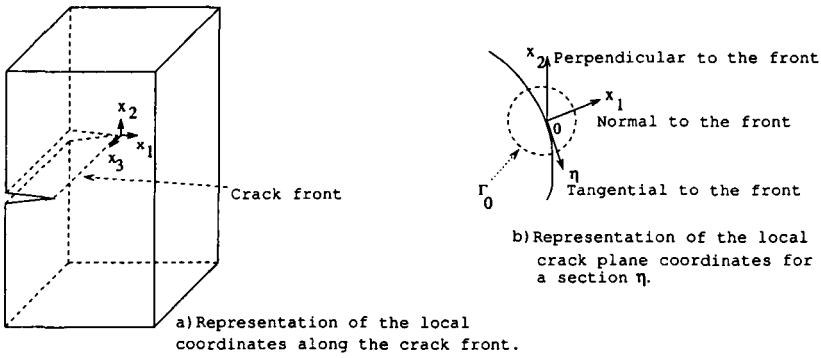

Figure 2. *Local coordinates along the crack front in 3-D*

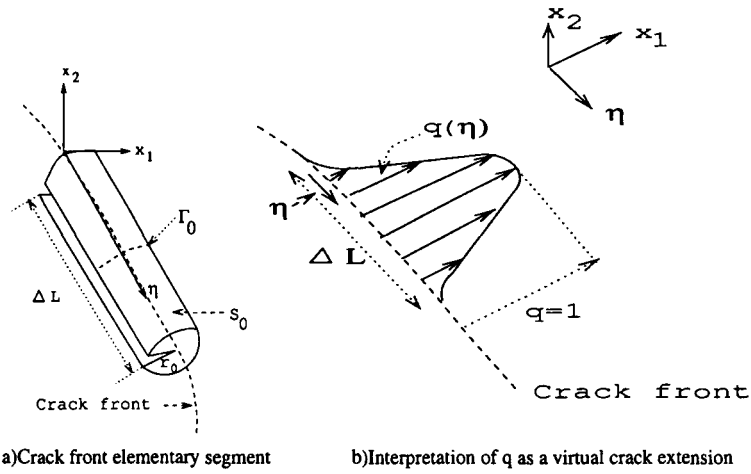

Figure 3. *Area enclosing an elementary segment of the crack front*

The q function is assimilated to a virtual crack extension of the point η in the direction normal to the crack front. ΔL is the length of the elementary segment under consideration (figure 3a). For each displacement $q(\eta)$ corresponds an increment of a potential energy $-\delta\pi = J(\eta)q(\eta)$. Let us note $-\delta\pi$ the total variation of the potential energy corresponding to the virtual extension of the whole segment ΔL (see figure 3b) we have:

$$-\delta\pi = \int_{\Delta L} J(\eta)q(\eta)d\eta \qquad [14]$$

We introduce $\overline{J}$ the energy corresponding to the extension of an elementary segment of the crack front, which makes it possible to write:

$$-\delta\pi = \overline{J}\triangle L = \int_{\triangle L} J(\eta)q(\eta)d\eta \qquad [15]$$

By replacing $J(\eta)$ by its expression, we obtain:

$$\overline{J}\triangle L = \lim_{r_0 \to 0} \int_{S_0} [W\delta_{1i} - \sigma_{ij}\frac{\partial u_j}{\partial x_1}]qn_i dA \qquad [16]$$

We construct around the tube of radius r_0 (see figure 3a) another tube of radius r_1 (see figure below), we define (as in the two-dimensional case) J for the new closed area, which results in the expression below:

$$\overline{J}\triangle L = \int_{S^*} [\sigma_{ij}u_{j,1} - W\delta_{1i}]qm_i dA \qquad [17]$$

where the area $S^* = S_1 + S^+ + S^- - S_0$ is as indicated in figure 4:

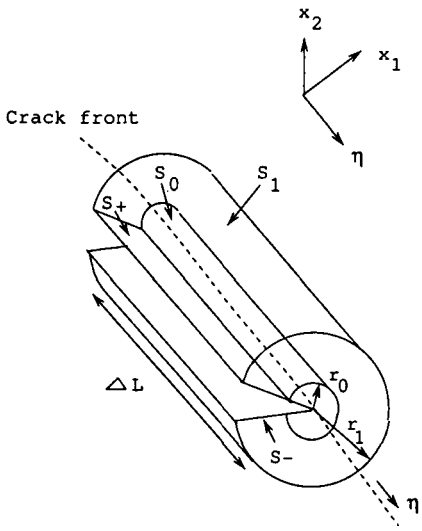

Figure 4. *The areas S_0 and S_1 enclosing the volume integration B^* in 3-D*

The definition of q is:

$$q = \{ \ 1 \quad \text{on} \quad S_0 \qquad \text{and} \qquad 0 \quad \text{on} \quad S_1 \ \} \qquad [18]$$

The three-dimensional formulation of the integral domain method is:

$$\overline{J}\triangle L = \int_{A^*} [\sigma_{ij} u_{j,1} - W\delta_{1i}] m_i q dA \qquad [19]$$

In this equation, we considered that :

$m_1 = 0$, $m_3 = 0$ and $m_2 = \pm 1$ on the crack faces supposed to be traction free. By applying the divergence theorem to the area integral of equation [19],

we obtain:

$$\overline{J}\triangle L = \int_{V^*} [\sigma_{ij} u_{j,1} - W\delta_{1i}] q_{,i} dB \qquad [20]$$

We have to combine this last expression with equation [15] to find out the pointwise value of J : $J(\eta)$. The result is (cf. Anderson [AND 91]):

$$J(\eta) = \frac{\overline{J}\triangle L}{\int_{\triangle L} q(\eta) d(\eta)} \qquad [21]$$

where the denominator term represents the variation of the area of the crack resulting from its virtual extension, this area is represented in the figure (3a).

5.2. *The case of a piezo-electrical material*

Theoretical development

Let us consider the general case i.e, the three-dimensional one, and let us adopt, first, a simplified mesh (figure 5a).

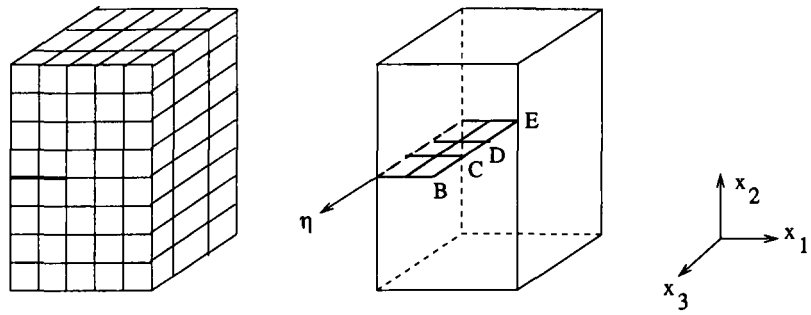

a) The 3-D mesh. b) The mesh along the crack front

Figure 5. *Path integral in 3-D*

We consider the axis "η" with origin "E" (figure 5b) along the crack front, as in the elastic case, we define in each point of the axis "η" (figure 5a) a path "Γ" which center is the point under consideration (that is the case for the point "D" in (figure 6a) and then we compute the J integral of which the expression is:

$$J(\eta) = \int_{\Gamma} (W\delta_{i1} - \sigma_{ij}u_{j,1} - D_i\phi_{,1})n_i d\Gamma \qquad [22]$$

For the point D, we can write $J_D = J(\eta_D)$. If we move virtually the point D in the "x_1" direction of a distance $\delta a(\eta_D)$, we obtain a potential energy variation:

$$-\delta\pi_D = J(\eta_D)\delta a(\eta_D) \qquad [23]$$

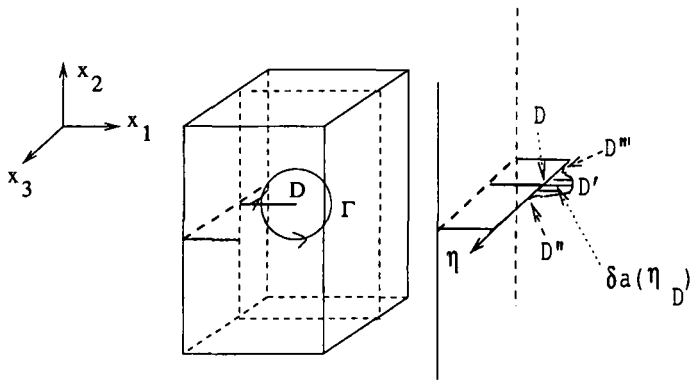

a)The integral J in D b)Result of the virtual extension of D

Figure 6. *Integral path J in the point D*

During its own extension, the D point carries away the points situated on the right of (D") and also the ones situated on the left of (D'''). D" and D''' are located respectively on the left and on the right of D on the (η) axis (see figure 6 b).

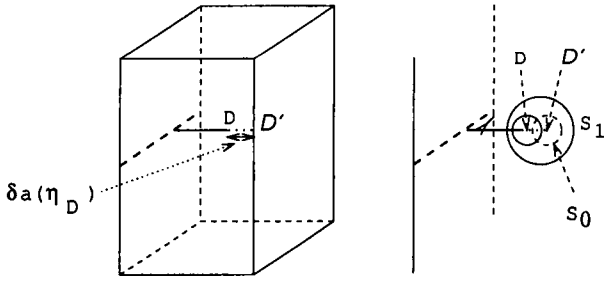

a)Virtual crack extension of D b)The area integral at D

Figure 7. *Virtual crack extension in 3-D*

If $\delta a(\eta)$ is the virtual extension of any point located along the segment $\eta_{D"D'''}$ and $J(\eta)$ is its corresponding path integral, then, the total change of potential energy of the material under consideration is:

$$-\delta\pi = \int_{\eta_{D"D'''}} J(\eta)\delta a(\eta)d\eta \qquad [24]$$

We note the distance $\eta_{D"D'''}$ by ΔL, if we introduce the released energy for a virtual extension of a unit segment of the crack front, we obtain:

$$\overline{J}\Delta L = -\int_A (W\delta_{1i} - \sigma_{ij}u_{j,1} - D_i\phi_{,1})m_i q dA \qquad [25]$$

A is any area enclosing the crack tip which can be represented, for example, by the lateral area A_1 of the cylinder of radius R_1 (see figure 8).

Let us consider the lateral area $A^* = A_1 + A^+ - A_0 + A^-$ and let us introduce the exterior normal to this area defined by:

– on A_0 : $m_i = -n_i$;

– on A_1 : $m_i = n_i$;

– on A^+ and A^- : $m_1 = 0$ and $m_2 = \pm 1$.

We introduce the q function defined by:

$$\begin{cases} q = 0 & \text{on} \quad A_1 \\ q = 1 & \text{on} \quad A_0 \end{cases} \qquad [26]$$

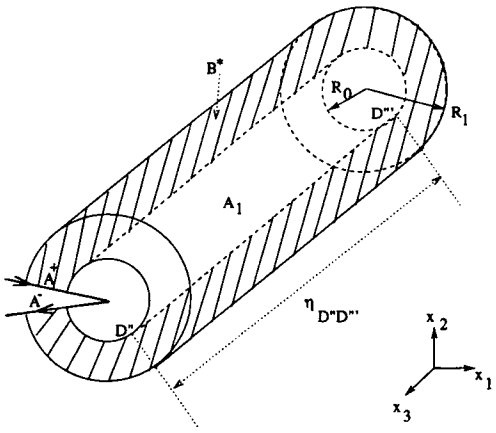

Figure 8. *The volume of integration in 3-D*

The integration along the area A_0 is the same as the one along A^*. The proof of this is as follows:

$$\overline{J}\triangle L = -\int_{A_0} (W\delta_{1i} - \sigma_{ij}u_{j,1} - D_i\phi_{,1})m_i q dA \qquad [27]$$

$$= -\int_{A_1+A^+-A_0+A^-} (W\delta_{1i} - \sigma_{ij}u_{j,1} - D_i\phi_{,1})m_i q dA$$

$$+ \int_{A_1} (W\delta_{1i} - \sigma_{ij}u_{j,1} - D_i\phi_{,1})m_i q dA$$

$$+ \int_{A^++A^-} (\sigma_{ij}u_{j,1} - D_i\phi_{,1}))m_i q dA \qquad [28]$$

The second term of the integral vanishes because q is taken equal to zero on A_1, the third term is also zero if we consider that the crack faces are traction free and that $D^+ = D^- = 0$. In this way we have proved that:

$$\overline{J}\triangle L = -\int_{A^*}(W\delta_{1i} - \sigma_{ij}u_{j,1} - D_i\phi_{,1})m_i q dA \qquad [29]$$

By using the divergence theorem we then obtain:

$$\overline{J}\triangle L = -\int_{B^*}\frac{\partial}{\partial x_i}[(W\delta_{1i} - \sigma_{ij}u_{j,1} - D_i\phi_{,1})q]dB. \qquad [30]$$

$$= -\int_{B^*}[(W\delta_{1i} - \sigma_{ij}u_{j,1} - D_i\phi_{,1})\frac{\partial q}{\partial x_i}$$

$$+ (\frac{\partial W}{\partial x_i} - \frac{\partial}{\partial x_i}(\sigma_{ij}\frac{\partial u_j}{\partial x_1} + D_i\frac{\partial \phi}{\partial x_1}))]dB \qquad [31]$$

If the body forces vanish, the second term of the integral vanishes as well. This makes it possible to write:

$$\overline{J}\triangle L = -\int_{B^*}(W\delta_{1i} - \sigma_{ij}u_{j,1} - D_i\phi_{,1})\frac{\partial q}{\partial x_i}dB \qquad [32]$$

Here B^* is the volume enclosed by the two cylinders of radius R_0 and R_1 of figure 8, and the virtual crack extension is in the x_1 direction. Figure (6b) shows that q on D" and $D"'$ (which corresponds to the ends of the cylinder of figure 8) is equal to "0".

In practice, R_0 is taken to be equal to zero, this means that the virtual extension is only applied to the crack tip. In this case, A^* corresponds to the lateral area of the cylinder of radius R_1 (figure 8).The pointwise value of J is $J(\eta)$ and its expression is given by equation 21.

6. Implementation of the numerical computation

We consider equation [32], by expanding this expression and arranging the different terms we obtain:

$$\overline{J}\triangle L = \int_{B^*}(\sigma_{11}u_{1,1} + \sigma_{12}u_{2,1} + \sigma_{13}u_{3,1} + D_1\phi_{,1} - W)\frac{\partial q}{\partial x_1}dB$$

$$+ \int_{B^*}(\sigma_{21}u_{1,1} + \sigma_{22}u_{2,1} + \sigma_{23}u_{3,1} + D_2\phi_{,1})\frac{\partial q}{\partial x_2}dB$$

$$+ \int_{B^*} (\sigma_{31}u_{1,1} + \sigma_{32}u_{2,1} + \sigma_{33}u_{3,1} + D_3\phi_{,1}) \frac{\partial q}{\partial x_3} dB$$

$$= J_1 + J_2 + J_3 \qquad [33]$$

Here q is given by equation [34], and $\frac{\partial q}{\partial x_j}$, where $j = \{1, 2 \text{ or } 3\}$, is given by the expressions [35]

$$q = \sum_{i=1}^{8} N_i q_i \qquad [34]$$

$$\frac{\partial q}{\partial x_j} = \frac{\partial \sum_{i=1}^{8} N_i q_i}{\partial x_j} = \sum_{i=1}^{8} \left(\frac{\partial N_i}{\partial \xi}\frac{\partial \xi}{\partial x_j} + \frac{\partial N_i}{\partial \eta}\frac{\partial \eta}{\partial x_j} + \frac{\partial N_i}{\partial \zeta}\frac{\partial \zeta}{\partial x_j}\right) q_i \qquad [35]$$

J_1, J_2 and J_3 represent the three integrals of the expression [33] and are calculated in the Gaussian points; the coordinates of the Gaussian points and the corresponding weights can be found in the book by Dhatt and Touzot [DHA 81] or in Zienkiewicz's [ZIE 71].

J can be calculated as follows:

$$\overline{J}\triangle L = \sum_{\xi_g=1}^{3} \sum_{\eta_g=1}^{3} \sum_{\zeta_g=1}^{3} (J_1 + J_2 + J_3) detC w_{\xi_g} w_{\eta_g} w_{\zeta_g} \qquad [36]$$

where ξ_g,η_g and ζ_g are the integration Gaussian points and w_{ξ_g}, w_{η_g} and w_{ζ_g} are the corresponding weights.

The example below can give us an idea about the choice of the value of q:

Let us consider the example of the mesh represented in figure 9a. The details of the mesh along the crack front are given in figure 9b. In the plane $(o, \vec{x_1}, \vec{x_2})$, $q = 1$ on S_0 and on the points located in the region enclosed by S_0 and S_1, $q = 0$ for the points situated on S_1.

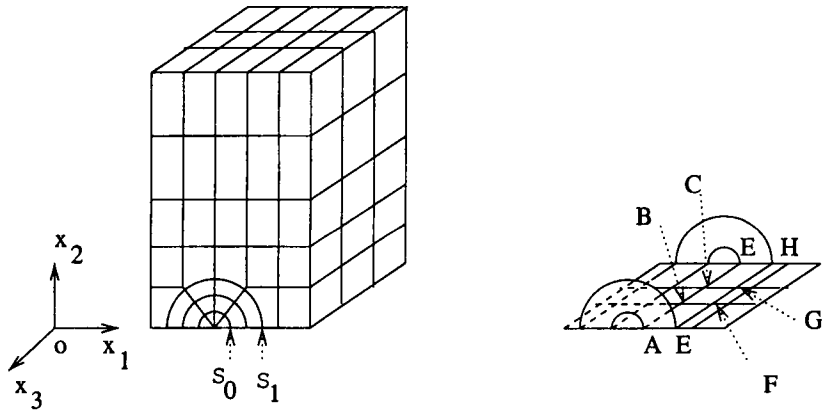

a) An example of a mesh in 3-D.

b) The ox 3x1 plan.

Figure 9. *Example of mesh in 3-D*

Along the x_3 axis, "$q = 1$" on the point where J is calculated and "0" in the adjacent points. If we consider a point situated in the end point, for example "E" (or "H"), "$q = 1$" for this point and "$q = 0$" for the point "F" ("G" if the point under consideration is "H"), for an internal point like "F" (or"G"),"$q = 1$" for the point under consideration and "$q = 0$" for the adjacent points. In this case the adjacent points are : "E" and "G" (i.e., "F" and "H" if we calculate J for the point "G").

7. Numerical results

7.1. *Introduction*

The authors mentioned here computed J by using an "approximated method". The most recent of these articles is the one written in 1995 by Park and Sun [SUN 95]. They presented the electrical and mechanical loadings for a piezoelectric material for each mode of fracture with the corresponding expression which leads to the computation of J (or G). This is summarized below.

For a PZT-4H piezoelectric ceramic, the total energy release rate (G) for each mode of fracture was obtained as:

$$G_I = \frac{1}{2}\pi \left[1.48 \times 10^{-11}\sigma_{33}^{\infty 2} + 2(2.67 \times 10^{-2}\sigma_{33}^{\infty} D_3^{\infty}) - 8.56 \times 10^{7} D_3^{\infty 2}\right] \quad [37]$$

$$G_{II} = \frac{1}{2}\pi \left[1.10 \times 10^{-11}\sigma_{13}^{\infty 2} + 2(2.59 \times 10^{-2}\sigma_{13}^{\infty} D_1^{\infty}) - 1.14 \times 10^{8} D_1^{\infty 2}\right] \quad [38]$$

$$G_{III} = \frac{\pi}{2(c_{44}\epsilon_{11} + e_{15}^2)}[\epsilon_{11}\sigma_{23}^{\infty 2} + 2(e_{15}\sigma_{23}^{\infty} D_2^{\infty}) - c_{44} D_2^{\infty 2}] \quad [39]$$

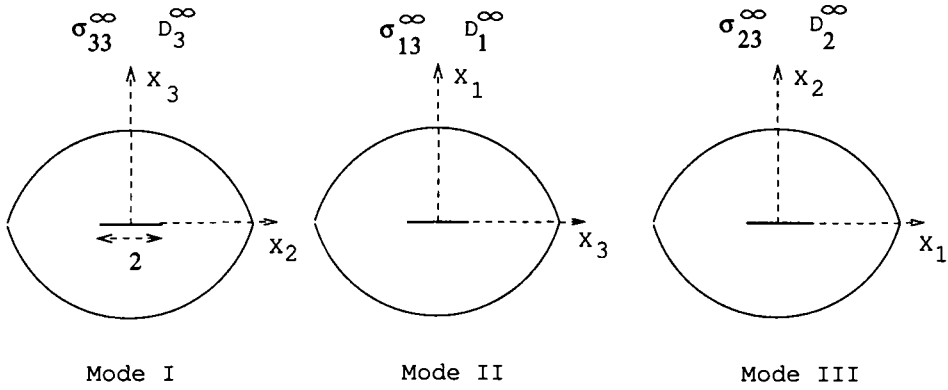

Figure 10. *The loading corresponding to each mode of fracture*

7.2. *Presentation of the example considered for the numerical computations*

In this section, we will consider a few examples of the fracture of a piezoelectric ceramic, for which the approximate computation of J is given in the corresponding article. The difference between the examples considered is the direction of the polarization axis in comparison with the position of the mechanical loading and crack front. This is a way to validate our numerical computation procedure on the one hand and to find out the variation of J in function of the variation of the electric potential on the other hand. The finite elements mesh used for the different examples is the same in all cases (see figure 11). This mesh represents half of the whole plate under consideration for an edge-cracked plate and quarter of the plate in the case of a central-cracked one (when the symmetry of the geometry and the loading is taken into account). The geometrical features (thickness, length and width) are left unchanged. We will consider the PZT-5H and PZT-4H which are the most used piezoelectric ceramics.

The properties of the PZT-5H are [PAK 92]:

$C_{11} = 12.6\ 10^{10}\ N/m^2$, $C_{12} = 5.5\ 10^{10}\ N/m^2$, $C_{13} = 5.3\ 10^{10}\ N/m^2$
$C_{33} = 11.7\ 10^{10}\ N/m^2$, $C_{44} = 3.53\ 10^{10}\ N/m^2$, $C_{66} = 3.55\ 10^{10} N/m^2$,
$e_{31} = -6.5\ C/m^2$, $e_{33} = 23.3\ C/m^2$, $e_{15} = 17\ C/m^2$,
$\epsilon_{11} = 151\ 10^{-10}\ C/Vm$, $\epsilon_{33} = 130\ 10^{-10}\ C/Vm$.

The properties of the PZT-4H are [SUN 95]:

$C_{11} = 13.9\ 10^{10}\ N/m^2$, $C_{12} = 7.78\ 10^{10}\ N/m^2$, $C_{13} = 7.43\ 10^{10}\ N/m^2$
$C_{33} = 11.3\ 10^{10}\ N/m^2$, $C_{44} = 2.56\ 10^{10}\ N/m^2$, $C_{66} = 3.06\ 10^{10}\ N/m^2$,
$e_{31} = -6.98\ C/m^2$, $e_{33} = 13.84\ C/m^2$, $e_{15} = 13.44\ C/m^2$,
$\epsilon_{11} = 6.\ 10^{-9}\ C/Vm$, $\epsilon_{33} = 5.47\ 10^{-9}\ C/Vm$.

For each example, the position of the crack front in the finite element mesh is represented in figure 11.

S_1, S_2 and S_3 in figure 11 correspond to the different areas where J is computed. J corresponds to $J(S_2)$ when the area is not indicated.

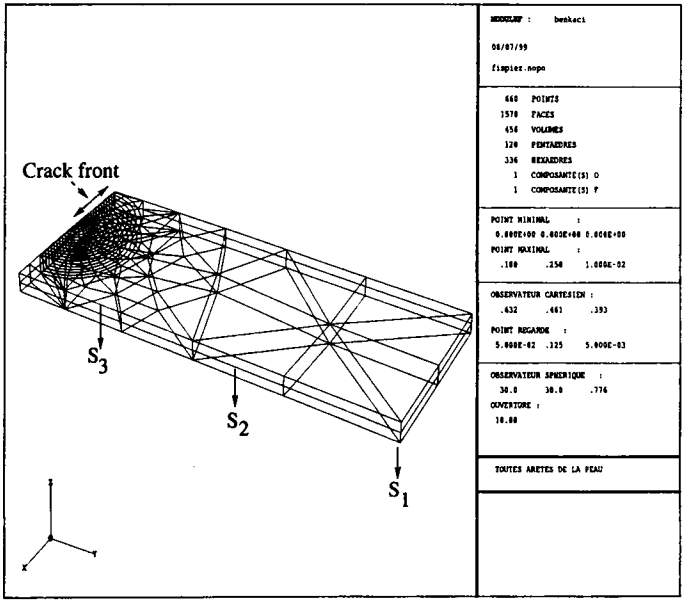

Figure 11. *The finite element mesh for a piezoelectric plate*

7.3. *Validation of the adopted numerical method*

In order to validate the numerical method presented above to compute J, we consider the case of the polarisation axis parallel to the crack front (direction x_3) and perpendicular to the mechanical loading. This example is the one studied by Suo *et al* in their article published in 1992 [SUO 92]. The manner in which the electrical and mechanical loadings are applied is shown in figure 13. Suo *et al* computed J by using the following equation

$$J = \frac{1}{2H}(C_{2222}\Delta^2 - \epsilon_{22}\phi^2 + 2e_{222}\phi\Delta) \qquad [40]$$

Figure 12 shows the computation results for $\Delta = 6\ \mu m$, and a variable ϕ for a PZT-4H ceramic. The curve "num" is the one obtained by using the energy domain integral method and the one referenced by "Suo" is the one obtained by using the expression [40] thanks to the mathematic program "MAPLE".

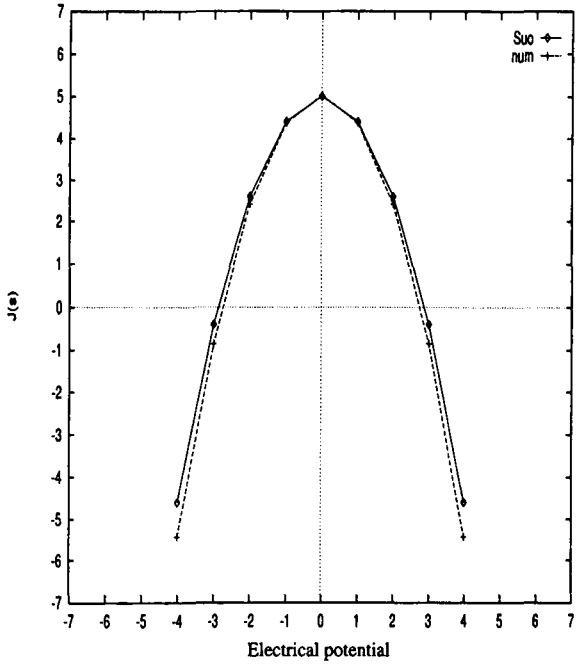

Figure 12. *$J = f(\phi)$ for a ceramic PZT-4H (J is in N/m and ϕ in $10^{-4}V$)*

The graph shows that the numerical results obtained are very satisfactory. Indeed, if we consider the difference in terms of the absolute value between the two values

J_{num} and J_{Suo}, we find out that for $\phi = 0\ V$, we have only 0.005 % of difference between the two values and 0.007 % for $\phi = 1\ 10^4\ V$. We can then conclude that our optimistic previsions concerning the utilization of the energy domain integral method for the computation of the J for a piezoelectric ceramic were right.

Let us take advantage of using a three-dimensional study to try to know the variation of J along the thickness. Some results are given in Table 1 (the considered units are, e : m, ϕ : $10^{+5}\ V$, $J : N/m$ and $\triangle = 6\mu m$).

Considering this table, we can note that for an external loading such as the one adopted by Suo et al, the J integral doesn't vary when the plate thickness varies; its value is almost the same for either 0.002 m or 0.01 m. For a given thickness, J is constant from one area to another. There is little variation for the area situated on the extremity of the plate, but its value is still close to the value of the area situated on the middle of the plate thickness.

Also the direction of electric field doesn't influence the crack propagation. Figure 12 shows that a negative electrical potential involves a negative J. In this case, the crack faces are in contact and J is taken to be equal to zero.

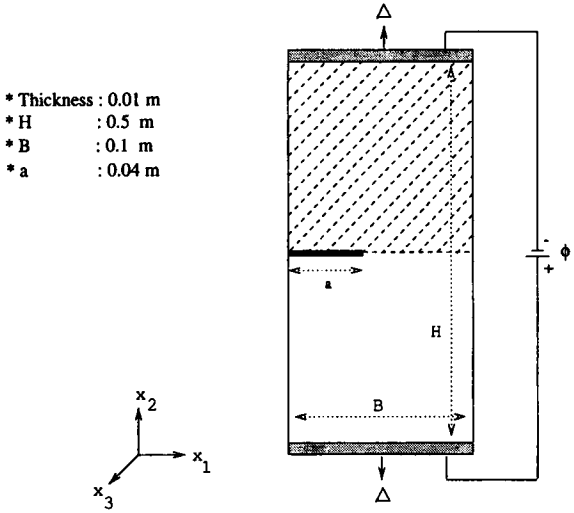

Figure 13. *The loading of a piezoelectric plate studied by Suo et al*

7.4. *Computation of J for the Mode III*

	$e = 0.002$	$e = 0.002$	$e = 0.002$	$e = 0.01$	$e = 0.01$	$e = 0.01$
	$\phi = -0.1$	$\phi = 0$	$\phi = 0.1$	$\phi = -0.1$	$\phi = 0$	$\phi = 0.1$
$J(s_1)$	4.3194	5.0093	4.4168	4.2985	4.9388	4.2733
$J(s_2)$	4.3748	5.0285	4.3749	4.3857	5.0393	4.3858
$J(s_3)$	4.4081	5.0254	4.3107	4.2736	4.9403	4.2987

Table 1. *Values of J along the thickness for the PZT 4H ceramic (s_1, s_2 and s_3 as indicated in figure 11)*

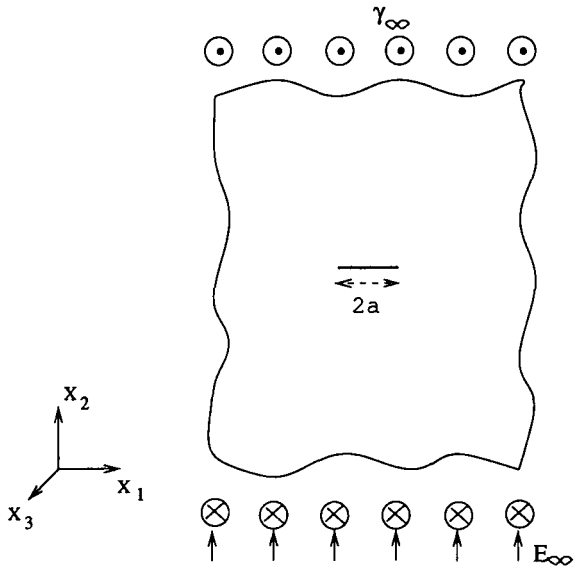

Figure 14. *Representation of the external loading for the Mode III*

In his article of 1990, Pak [PAK 90] considered a loading like the one represented in figure 14 (the geometrical characteristic parameters are the same as those given in figure 13), with a polarisation axis following the x_3 direction and parallel to the crack front (which also follows x_3) and to the external mechanical loadings.

Pak has calculated the crack force extension for a PZT-5H piezoelectric ceramic by using the following expression:

$$J = \frac{\pi\, a}{2}[c_{44}\, \gamma_\infty^2 - \epsilon_{11}\, E_\infty^2 - 2\, e_{15}\, E_\infty \gamma_\infty] \qquad [41]$$

We have calculated J numerically by using the energy domain integral for the same problem. We have noted the corresponding value $J(num)$, and then we compared $J(num)$ to the value obtained by expression [41] computed by using the "MAPLE" program. We have then compared the difference (in absolute value) between $J(num)$

and $J(Pak)$ (the unit of J is N/m) for three values of E_∞ (E_∞ is in 10^{+4} V/m, $\gamma_\infty = 2.375\ 10^{-5}$ and $e = 1\ cm$). The results are given in Table 2 which shows, once again, the efficiency of the numerical method.

E_∞	$J(Pak)$	$J(num)$	error
-0.5	5.4879	5.3175	3.1 %
0	5.0043	4.9575	0.94 %
0.5	4.4732	4.3312	3.2 %

Table 2. *Comparison of the numerical and theoretical results for the example studied by Pak*

For $\gamma_\infty = 2.375\ 10^{-5}$, $e = 1\ cm$ and for two different materials, we tried to know the variation of J in function of the electric potential. We obtained figure 15 which first shows that for a PZT-5H piezoceramic J is larger than the PZT-4H one. This is quite normal because of the larger value of the PZT-5H coefficients compared to the PZT-4H ones, especially the c_{44} coefficient of which value is $3.53\ 10^{10}$ while for PZT-4H its value is only $2.56\ 10^{10}$. J_{max} is reached for $\phi_{max} = 0.5\ 10^4\ V$ for a PZT-5H and for a PZT-4H, $J_{max}$is obtained for $\phi_{max} = 0.75\ 10^4\ V$. For a negative value of the electric potential, we have a negative value for J for both materials. This means that the two crack faces are in contact and in reality, J is taken to be equal to zero. In this case and in the case of an electric potential larger than ϕ_{max}, it will not have any crack propagation. For a value of an electric potential situated between zero and ϕ_{max}, the crack propagation will be facilitated by the electrical field. We can explain this by the fact that the applied electrical field is shared between the elastic stress and the electric induction. Between zero and ϕ_{max} the induction is weak compared to the stress, this fact has caused the crack propagation. For an electric potential larger than ϕ_{max}, the induction effect becomes preponderant over the stress one. This results in the stop of the crack propagation.

	$e = 0.002$	$e = 0.002$	$e = 0.002$	$e = 0.01$	$e = 0.01$	$e = 0.01$
	$\phi = -0.1$	$\phi = 0$	$\phi = 0.1$	$\phi = -0.1$	$\phi = 0$	$\phi = 0.1$
$J(s_1)$	-1.9516	0.7994	-0.9897	2.3598	7.4287	8.4619
$J(s_2)$	0.5006	4.2526	3.6360	0.8504	4.9575	4.7949
$J(s_3)$	-0.4879	0.7994	-0.9897	2.3598	7.4287	8.4619

Table 3. *Values of J along the thickness for a PZT-5H ceramic*

The three-dimensional calculation leads to an evaluation of the variation of J along (and in function of) the thickness. The results are given in Table 3 (the considered units are, e : m, ϕ : 10^{+5} V, J : N/m, and $\gamma_\infty = 2.375\ 10^{-5}$) where we can see that the $J(s_2)$ value, which corresponds to the middle of the plate, does not differ much whether we consider $e = 0.002$ or $e = 0.01\ m$. On the other hand, because the polarisation axis is along the thickness, the J value differs from one area to another.

J can either increase or decrease in the end points of the plate. It depends on the sign of the applied electrical potential.

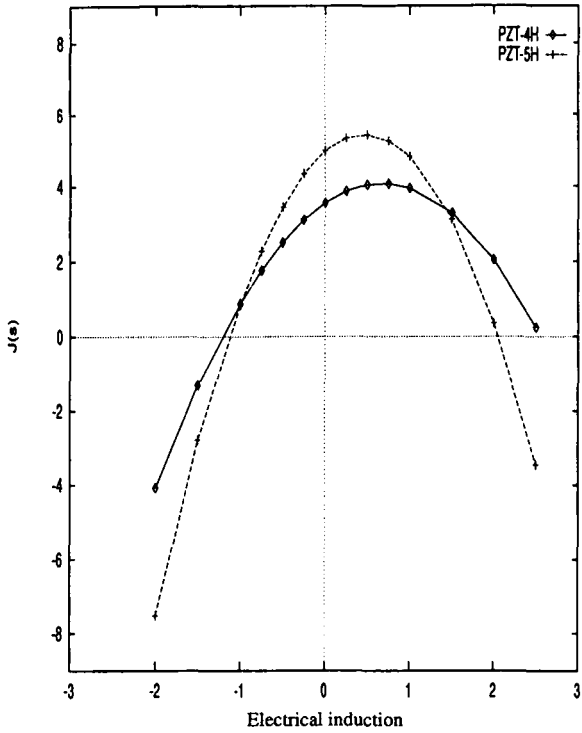

Figure 15. *$J = f(\phi)$ for the Mode III (J is in N/m and ϕ in 10^4 V)*

For the mechanical loading (with $\phi = 0.1\ 10^5\ V$ and $e = 1\ cm$), figure 16 shows that it always increases J which implies the crack propagation.

7.5. *Calculation of J for the Mode I*

Let us consider the loading considered by Park and Sun [SUN 95] which is represented in figure 17. The material is placed so that its polarisation axis (which is along the x_3 axis) is perpendicular to the crack front. In this case, crack prapagation will be along the x_2 axis.

The finite element mesh used is represented in figure 19. Because of the change of the crack propagation direction, we write J in the following manner:

$$\overline{J}\triangle L = \int_{B^*} [(\sigma_{ij} u_{j,2} + D_i \phi_{,2} - W\delta_{i2}) \frac{\partial q}{\partial x_i}] dB \qquad [42]$$

For the computation of J, Park and Sun used the following expression

$$G_I = \frac{1}{2}\pi \left[1.48 \times 10^{-11} \sigma_{33}^{\infty 2} + 2(2.67 \times 10^{-2} \sigma_{33}^{\infty} D_3^{\infty}) - 8.56 \times 10^{7} D_3^{\infty 2}\right] \qquad [43]$$

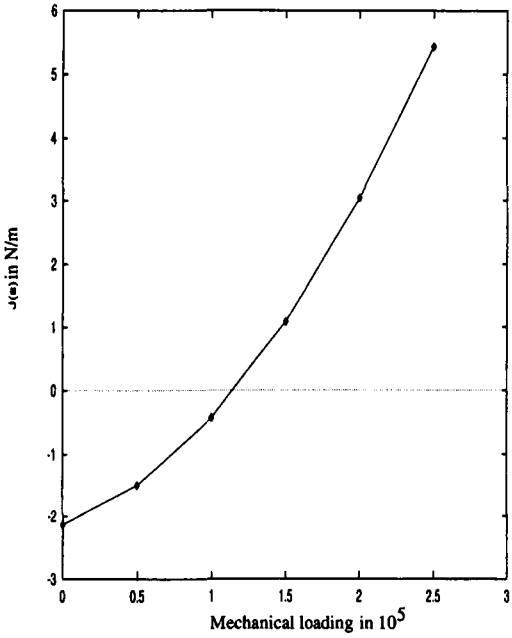

Figure 16. *$J = f$(mechanical loading) for a PZT-4H ceramic*

	$\phi = -0.1\ 10^4$	$\phi = -0.1\ 10^3$	$\phi = 0.$	$\phi = 0.5\ 10^3$	$\phi = 0.1\ 10^4$
J_{theo}	10.8739	10.8120	10.7498	10.6872	10.6243
J_{num}	10.3813	10.3811	10.3757	10.3644	10.3478
|error|	4.53 %	3.99 %	3.48 %	3.02 %	2.6 %

Table 4. *Numerical and theoretical results for a PZT-4H ceramic loaded in a I mode*

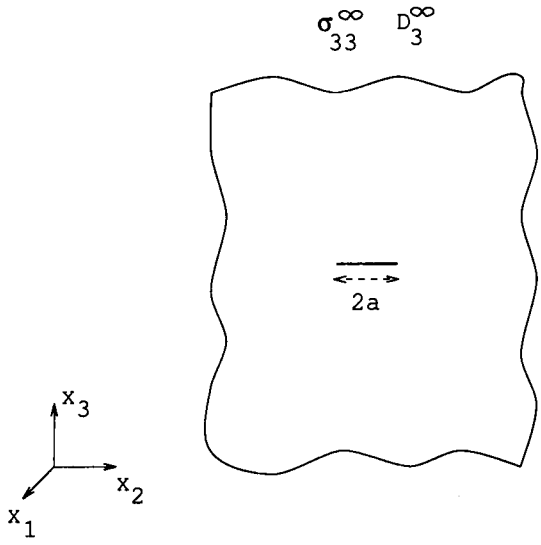

Figure 17. *The piezoelectric plate loading in Mode I*

ϕ	$J(PZT-4H)$	$J(PZT-5H)$
0	10.3837	8.0611
$-0.25\ 10^3\ V$	10.3872	8.0620
$-1\ 10^3\ V$	10.3895	8.0482

Table 5. *The ϕ values for which J is maximal for the PZT-4H and PZT-5H ceramics*

We have calculated J numerically by using the energy domain integral for the same problem for a PZT-4H ceramic, with an electric potential as an external loading and a stress equal to $3.4\ 10^6\ Pa$. We denoted the results obtained as J_{num} and compared the results to those obtained by [43] using the "MAPLE" program. The results obtained are denoted as J_{theo}.

The difference between the two computations is given in Table 4 (ϕ is in V and J in N/m and $e = 1\ cm$) which shows, once again, the validity of the numerical method we used.

By choosing the external electric loading values, equivalent to those used by Park and Sun and for two different thicknesses ($e = \{0.002, 0.01\}\ m$) and for a stress equal to $3.4\ 10^6\ Pa$, we have drawn in figure 18 the variation of J in function of the electric potential for a PZT-4H ceramic and in figure 20 the one corresponding to a PZT-5H ceramic. As in the mode III, the curve is almost the same for both materials. The two curves also show that J does not vary whether we consider the thickness 0.002 or 0.01 m. In the neighborhood of $\phi = 0$, the values are very close. In order to see more clearly what happens in this zone, we have given the J values in table 5.

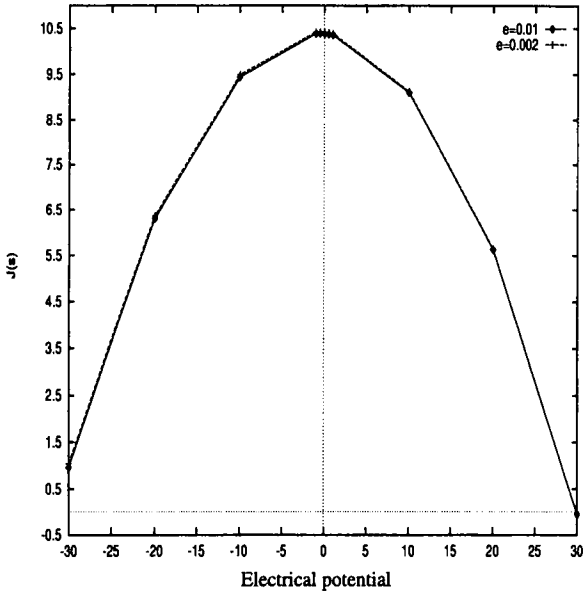

Figure 18. *$J = f(\phi)$ for a PZT-4H ceramic in Mode I (J is in N/m and ϕ in 10^3 V)*

From the table 5, we can see that J_{max} does not correspond to $\phi = 0$ but to $\phi = -10\ 10^3\ V$ for the PZT-4H ceramic and for the PZT-5H ceramic we have $\phi_{max} = -0.25\ 10^3\ V$. The two curves show that for a negative electric potential smaller than ϕ_{max}, the J value is negative, the crack faces are in contact, and in reality J is taken to be equal to zero. For an electric potential value smaller than ϕ_{max} and larger than zero, there will be no crack propagation. For an electric potential value between zero and ϕ_{max}, because of the stress which receives a contribution from the electric potential that increases its value, J increases and there is a tendency to a crack prapagation.

For an electric potential smaller than ϕ_{max} and larger than zero, when ϕ decreases (we are dealing with negative values), the electric induction effect becomes larger than that of the stress and the crack does not propagate any more.

We have studied the variation of J along the thickness for the PZT-5H ceramic. The results are given in Table 6 (the units used are e : in m, J : N/m and $\sigma_{33}^{\infty} = 3.4\ 10^6\ Pa$) where we can see that J does not vary a lot. This could be expected, because in this case the polarisation axis is not set along the thickness as was the case in the mode III.

The curve representing the variation of J in function of the mechanical loading is given in figure 21 (for a PZT-4H ceramic with $e = 1\ cm$ and $\phi = 0.1\ 10^4\ V$). We can see that J increases as the mechanical loading increases.

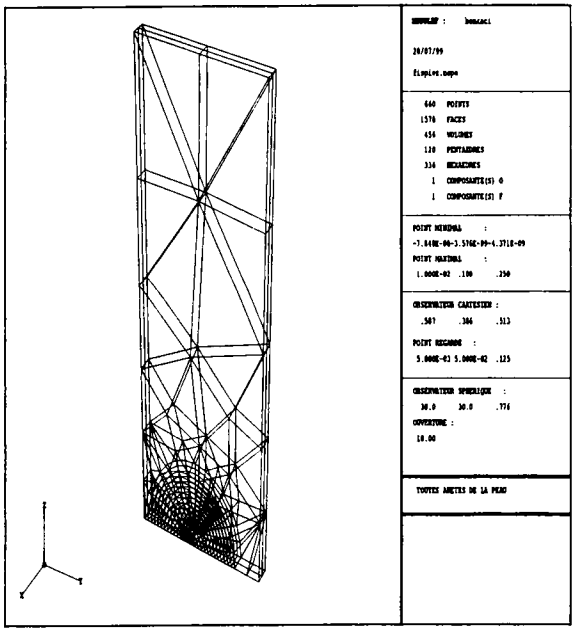

Figure 19. *The used mesh in Mode I*

	$e = 0.01$	$e = 0.01$	$e = 0.01$
	$\phi = 0$	$\phi = 0.5\ 10^3\ V$	$\phi = -0.5\ 10^3\ V$
$J(s_1)$	8.0376	8.0281	8.0364
$J(s_2)$	8.0505	8.0407	8.0495
$J(s_3)$	8.0374	8.0279	8.0359

Table 6. *The J values along the thickness for a PZT 5H ceramic.*

7.6. *Conclusion*

After computing J for a piezoelectric ceramic, we can conclude that:
i- The energy domain integral is suitable for the numerical computation of J.
ii- An exterior mechanical loading always enhances the crack propagation.
iii- An external electric loading can enhance or stop the crack propagation, depending on the crack mode, the loading and the direction of the polarisation axis.
iv- J varies along the thickness, when the polarisation axis is along the thickness. When the polarisation axis is not along the thickness, then J does not vary along the thickness.

These remarks are based on our own calculations. They need to be completed and supported by an experimental study.

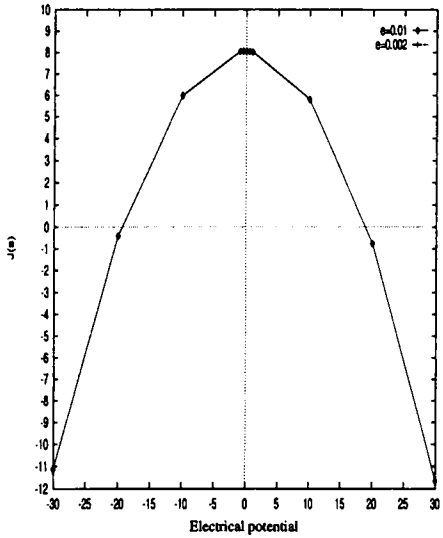

Figure 20. *$J = f(\phi)$ for a PZT-5H in mode I (ϕ is in 10^3 V and J in N/m)*

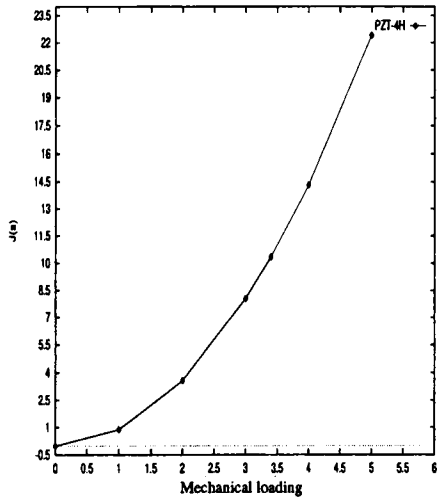

Figure 21. *$J = f(\text{mechanical loading})$ (J is in N/m and σ_{33} in 10^6 Pa)*

8. References

[AND 91] ANDERSON T.L., "Fracture mechanics fundamentals and application ", CRC PRESS, BOSTON, 1991.

[DAS 94] DASCALU C. , MAUGIN G.A., "Energy-release rates and path independent integrals in electroelastic crack propagation", *International Journal of Engineering Sciences*, vol. 32, 1994, p. 755-765.

[DAS 95] DASCALU C. , MAUGIN G.A., "On the energy of electric fracture", *Z angew Mathematics and Physics*, vol. 46, 1995, p. 355-365.

[DEE 80] DEEG W.F., "The analysis of dislocation, crack and inclusion problems in piezoelectric solids ", 1980, Stanford University, Stanford, California.

[CHU 89] CHUNG H.T. , SHIN, KIM, *Journal of American Ceramics Society*, vol. 72, 1989, p. 327.

[DHA 81] DHATT G., TOUZOT G., "Une présentation de la méthode des éléments finis", MALOINE S.A, 1981, LES PRESSES DE L'UNIVERSITÉ LAVAL, QUEBEC.

[MAU 93] MAUGIN G.A., "Material inhomogeneities in elasticity ", *Chapman & Hall, London*, 1993.

[MAU 95] MAUGIN G.A., "Material forces: concepts and applications", *Applied Mechanics Reviews*, vol. 48, 1995, p. 213-245.

[MCM 87] MCMEEKING R.M., *International Journal of Solids and Structures*, vol. 62, 1987, p. 3116.

[MCM 90] MCMEEKING R.M., "Integral for the analysis of electrically induced mechanical stress at cracks in elastic dielectrics ", *International Journal of Engineering Sciences*, vol. 28, 1990, p. 605-613.

[MIK 90] MIKHAILOV G.K. , PARTON V.Z., "Electromagnetoelasticity ", ,HEMISPHERE,NEW-YORK, 1995.

[PAK 90] PAK Y.E., "Crack extension force in a piezoelectric material", *Journal of Applied Mechanics*, vol. 57, 1990, p. 647-653.

[PAK 86] PAK Y.E. , HERMANN G., "Conservation laws and the material momentum tensor for the elastic dielectric ", *International Journal of Engineering Sciences*, vol. 24, 1986, p. 1365-1374.

[PAK 92] PAK Y.E., "Linear electroelastic fracture mechanics of piezoelectric materials ", *International Journal of Fracture*, vol. 54, 1992, p. 79-100.

[PAR 95] PARTON V.Z., "Fracture mechanics of piezoelectric materials ", *Acta Astronautica*, vol. 3, 1995, p. 671-683.

[RIC 71] RICE J.R., "A path-independent integral and the approximation analysis on strain concentration by notches and cracks ", *Journal of Applied Mechanics*, vol. 35, 1968, p. 379-386.

[SUN 95] SUN C.T. , PARK S.B., "Effect of electric field on fracture of piezoelectric ceramics", *International Journal of Fracture*, vol. 70, 1995, p. 203-216.

[SUO 92] SUO , KUO C.M., BARNETT D.M., WILLIS J.R., "Fracture mechanics for piezoelectric ceramics", *Journal of Mechanics and Physics of Solids*, vol. 40, 1992, p. 39-765.

[TON 96] TONG-YI ZANG , PPIN TONG, "Fracture mechanics for a mode III crack in a piezoelectric material ", *International Journal of Solids and Structures*, vol. 33, 1996, p. 343.

[ZIE 71] ZIENCKIEWICZ O.C., "The finite element method in engineering sciences", MC GRAW HILL , London, 1971.